NUCLEAR SCIENCE AND TECHNIQUES **26**, 060404 (2015)

An algorithm for ^{252}Cf-Source-Driven neutron signal denoising based on Compressive Sensing*

LI Peng-Cheng (李鹏程),† WEI Biao (魏彪), FENG Peng (冯鹏), HE Peng (何鹏), and MI De-Ling (米德伶)

Key Laboratory of Opto-electronics Technology and System,

Ministry of Education, Chongqing University, Chongqing 400044, China

(Received December 24, 2014; accepted in revised form March 6, 2015; published online December 20, 2015)

As photoelectrically detected ^{252}Cf-source-driven neutron signals always contain noise, a denoising algorithm is proposed based on compressive sensing for the noised neutron signal. In the algorithm, Empirical Mode Decomposition (EMD) is applied to decompose the noised neutron signal and then find out the noised Intrinsic Mode Function (*IMF*) automatically. Thus, we only need to use the basis pursuit denoising (BPDN) algorithm to denoise these *IMF*s. For this reason, the proposed algorithm can be called EMDCSDN (Empirical Mode Decomposition Compressive Sensing Denoising). In addition, five indicators are employed to evaluate the denoising effect. The results show that the EMDCSDN algorithm is more effective than the other denoising algorithms including BPDN. This study provides a new approach for signal denoising at the front-end.

Keywords: ^{252}Cf-source-driven neutron signal, Empirical mode decomposition, Compressive sensing, Denoising

DOI: 10.13538/j.1001-8042/nst.26.060404

I. INTRODUCTION

The photoelectric detection and imaging technology have been widely used in Nuclear Material Identification System (NMIS) to detect neutron signal and nuclear components. Time-frequency method has been used to analyze neutron signal and identify properties of nuclear material [1, 2], while tomographic imaging has been used to provide more information about geometry of nuclear components, which leads to high accuracy of NMIS [3–5]. However, it is inevitable that there are noises in the measurement process due to external environment, detector and electronic device, and the noises may confuse some useful but weak information. Thus, we should denoise the neutron signals first to improve accuracy of NMIS.

Except the circuit and technic neutron signal denoising methods, traditional denoising algorithms mostly represent the noised signal in transform domain and then threshold for the purpose of denoising. As a result, FFT filter and wavelet shrinkage has been applied in neutron signal denoising [6]. Besides, a new denoising algorithm named EMDSD (Empirical Mode Decomposition Double Smoothness Detecting) has been proposed for neutron signal [7]. However, these denoising algorithms cannot adjust decomposition base automatically.

In recent years, the paradigm of sparse sampling and reconstruction, called compressive sensing (CS), is a state-of-the-art research [8, 9]. CS approaches have opened up many new research avenues in the field of under-determined systems, and found many practical applications in image processing, wireless communication, data-streaming, and medical resonance. Also, CS has been applied in image denoising [10–14], and some new denoising algorithms [15, 16] are derived from basis pursuit denoising (BPDN) algorithm [17]. Although these algorithms are proposed for all signal frequency, the compressive reconstruction error will still increase and signal may be noised again.

Fortunately, the Empirical Mode Decomposition (EMD) can decompose the signal into Intrinsic Mode Function (*IMF*), from finer temporal scales (high frequency *IMF*s) to coarser ones (low frequency *IMF*s). As the noise is always in high frequency *IMF*s, BPDN algorithm can be adopted to denoise them. In this paper, we propose a new denoising algorithm named EMDCSDN (Empirical Mode Decomposition Compressive Sensing Denoising). Several denoising algorithms are compared with EMDCSDN algorithm to verify its robustness.

II. METHODOLOGY

A. Materials

Neutron signals from ^{252}Cf-source-driven nuclear material fission are detected by photoelectric detectors. We designed a ^{252}Cf-source-driven verification system to identify properties of ^{235}U (Fig. 1(a)). It consists of a ^{252}Cf neutron source, an ionization chamber, scintillation neutron detectors, workstation with high-speed (1 GHz) data acquisition card with a large-capacity disk array, verification software and user interface (UI) system. Three detectors are placed around the fissile material. The target-detector distance d and the angle α between detectors can be adjusted according to the measurement requirements (Fig. 1(b)).

Figure 2 shows the noised neutron pulse signal acquired by the ^{252}Cf-source-driven verification system. For experiment purpose, the EMDCSDN algorithm is adopted to denoise this signal. As the pure neutron signal is unknown, the curve fitting of noised neutron signal is regarded as the pure signal, so as to evaluate the denoising effect. All the materials are used without further purification.

* Supported by the National Natural Science Foundation of China (Nos. 61175005 and 61401049)

† Corresponding author, cqujwclpc@163.com

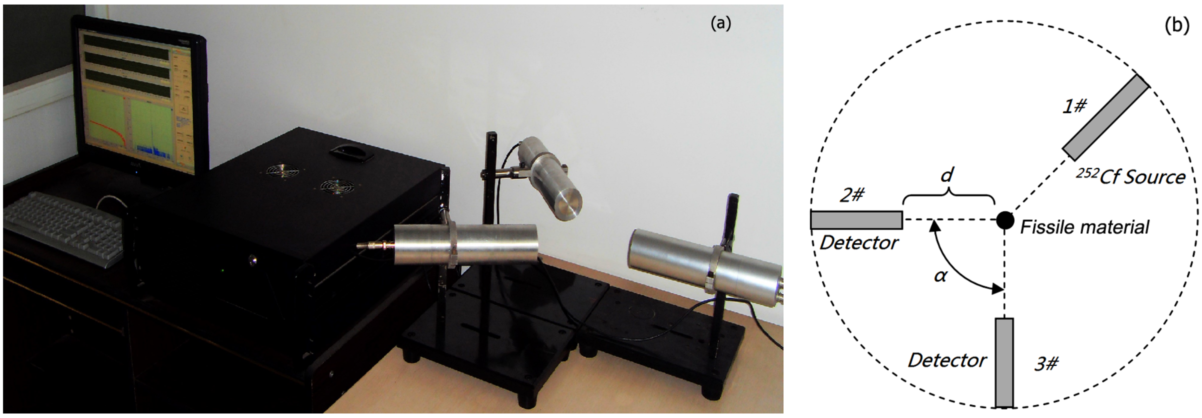

Fig. 1. (Color online) Prototype of ^{252}Cf-source-driven verification system (a) and position of detectors (b).

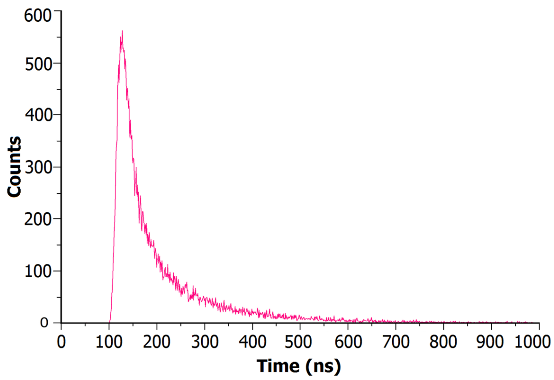

Fig. 2. (Color online) The noised neutron signal.

B. Basis pursuit denoising

Compressive sensing, the paradigm of sparse sampling and reconstruction, is an advanced theory. Specifically, let $\boldsymbol{x}= \{x_1, x_2, \ldots, x_N\}, \boldsymbol{x}\in R^N$ with $\boldsymbol{x}= \Psi\alpha$, where α has only K non-zero elements and $K \ll N$. The $\boldsymbol{x}$ is called as K-sparse with respect to the transform Ψ. So the random measurements $\boldsymbol{y}= \{y_1, y_2, \ldots, y_N\}, \boldsymbol{y}\in R^M$ are generated by

$$\boldsymbol{y} = \boldsymbol{\Phi x}, \quad \text{where } \boldsymbol{\Phi} \in R^{M\times N}, \tag{1}$$

where, $\boldsymbol{\Phi}$ is a randomly sampling matrix, and the number of measurement $M \ll N$. It is an ill-posed problem recovering $\boldsymbol{x}$ from $\boldsymbol{y}$. In the compressive sensing theory, it testifies that K-sparse signal $\boldsymbol{x}$ can be recovered by $M = O[K \log(N/K)]$ measurements as long as $\boldsymbol{\Phi}$ satisfies the restricted isometry property (RIP), and the reconstruction can be achieved with probability close to one by solving the following convex optimization.

$$\alpha = \arg\min \|\alpha\|_1, \quad \text{subject to } \boldsymbol{y} = \boldsymbol{\Phi}\psi\alpha, \tag{2}$$

where $\|\alpha\|_1$ denotes the l_1-norm of the vector α.

Thus, the compressive sensing process of neutron signal can be described as follows. It assumes that the noised neutron signal $\boldsymbol{x}= s + n = \psi\alpha + n$, where s is the original signal, n denotes additive Gaussian white noise and ψ is the sparse basis. Consequently, the compressive sampling can be defined as,

$$\boldsymbol{y} = \boldsymbol{\Phi}(s + n) = \boldsymbol{\Phi}s + \boldsymbol{\Phi}n = \boldsymbol{\Phi}s + z = \boldsymbol{\Phi}\psi\alpha + z, \tag{3}$$

where z is the noise in sampling and $\|z\|_2 \leq \varepsilon$.

The reconstruction can be achieved by Eq. (2). With noisy or imperfect data, it is impossible to fit the linear system exactly. Instead, the constraint in BP is relaxed to obtain the basis pursuit denoising problem.

$$\min_{\alpha} \|\alpha\|_1 \quad \text{subject to } \|y - \Phi\psi\alpha\|_2 \leq \varepsilon. \tag{4}$$

Therefore, an effective algorithm using Spectral Projected Gradient (SPG) is used to solve BPDN [17]. It can solve the BPDN problem much more quickly, and the memory requirements are constant throughout all the iterations. However, most of the noised signal frequencies are pure and there is no need to denoise them. So, if we use the BPDN algorithm for all frequencies, the signal will be noised again and some useful information may be filtered. Therefore, based on compressive sensing, a new denoising algorithm for the noised frequencies only is proposed.

C. EMDCSDN algorithm

Hilbert-Huang Transform (HHT) is a new method of time-frequency analysis technique, which was proposed by Huang [18], and the essence of this method is EMD. The EMD is advantageous in that the base functions are derived from the signal itself. Hence, the analysis is more adaptive, in contrast to the wavelet method where the base functions are fixed. Any signal can be decomposed into a finite and a small number of *IMF*s to give meaningful instantaneous frequency, as described by Eq. (5).

$$\boldsymbol{x} = \sum_{i=1}^{N} IMF_j + res, \tag{5}$$

where *res* means a residual of EMD.

Figure 3 shows the *IMF*s of neutron signal decomposed by EMD. It seems that only the first few high frequencies of *IMF*s are noised, and rest of the *IMF*s are pure. Although the EMD itself has characteristics of filter, the noised *IMF*s cannot be filtered directly. Therefore, we need to find the noised IMFs, to use BPDN algorithm for denoising.

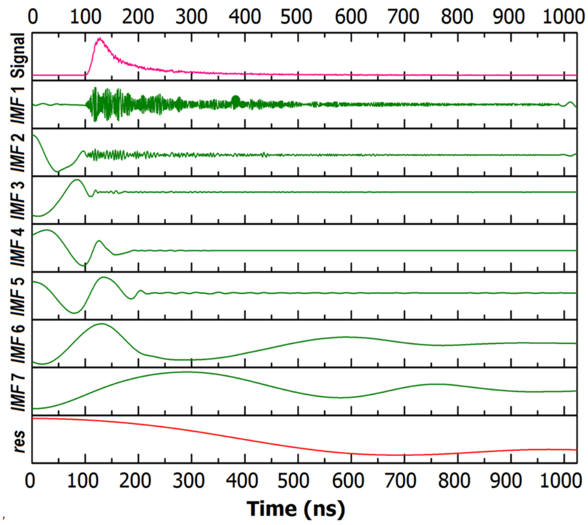

Fig. 3. (Color online) IMFs of neutron signal decomposed by EMD.

Thus, the EMDCSDN algorithm is proposed as shown in Fig. 4.

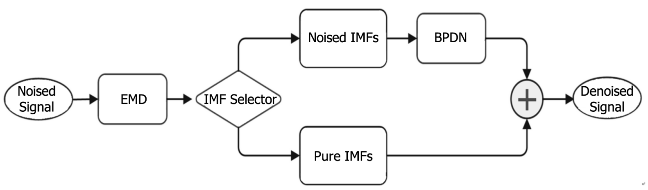

Fig. 4. The EMDCSDN algorithm.

Algorithm 1: EMDCSDN algorithm for neutron signal

Input: noised neutron signal x;
Output: denoised neutron signal x_D;
Decompose x to *IMF*s ($IMF_j, j = 1, 2, \ldots, N$) and *res*;
Select the noised *IMF*s($IMF_c, c = 1, 2, \ldots, C$) and pure *IMF*s($IMF_p, p = 1, 2, \ldots, P$) by *IMF* selector, where $N = C + P$;
Use BPDN algorithm to denoise the noised *IMF*s, and the output denoised *IMF*s are $D\_IMF_c, c = 1, 2, \ldots, C$;
Calculate $x_D = \sum_{c=1}^{C} D\_IMF_c + \sum_{p=1}^{P} IMF_p + res$;

In this EMDCSDN algorithm, the *IMF* selector is designed according to the characteristics of white noise [19]. One of the characteristics is that $\Gamma_i = E_i P_i$ is a constant, where E_i is the energy density and P_i is period of the *IMF*s.

$$E_i = \frac{1}{N}\sum_{j=1}^{N}[C_i(j)]^2, \quad P_i = \frac{2N}{n_{\max}(i) + n_{\min}(i)}, \tag{6}$$

where, N, C, $n_{\min}$ and $n_{\max}$ are the length, amplitude, the number of maxima and the number of minima of the *IMF*s, respectively.

If $R_i = |(\Gamma_i - \bar{\Gamma})/\bar{\Gamma}| \geq 1$, then $\Gamma_j(j = 1, 2, \ldots, i-1)$ is a constant and the first $i-1$ *IMF*s are noised, where $\bar{\Gamma}$ is the mean of Γ_j. Thus, we can use this *IMF* selector to find out which *IMF* is noised. Figure 5 shows that $R_3 > 1$, so for the noised neutron signal, IMF_1 and IMF_2 need to be denoised. Thereby, the EMDCSDN algorithm can narrow the denoising scope and reduce the compressive sensing reconstruction error, and the denoising effect will be improved. In the next section, how to evaluate the denoising effect will be discussed.

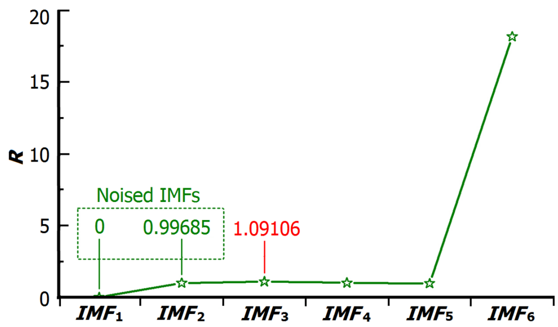

Fig. 5. (Color online) The *IMF* selector results of neutron signal.

D. Denoising evaluation

In general, the signal-to-noise ratio (SNR), peak signal-to-noise ratio (PSNR) and mean squared error (MSE) are adopted to evaluate the denoising effect. However, only the three indicators are not enough because high SNR means that some useful information has been filtered. So, another two indicators, smoothness of curve (*SOC*) and correlation coefficient (*CC*) should also be involved. The *SOC* and *CC* can be defined as:

$$SOC = \frac{\sum_{i=1}^{N-1}[\hat{x}(i+1) - \hat{x}(i)]^2}{\sum_{i=1}^{N-1}[x(i+1) - x(i)]^2}, \tag{7}$$

$$CC = \frac{\sum_{i=1}^{N}(x_i - \bar{x})(\hat{x}_i - \bar{\hat{x}})}{\sqrt{\sum_{i=1}^{N}(x_i - \bar{x})^2 \cdot \sum_{i=1}^{N}(\hat{x}_i - \bar{\hat{x}})^2}}, \tag{8}$$

where x is the original noised signal and $\hat{x}$ is the denoising signal. For *CC* indicator, the bigger the better. However, for *SOC* indicator, smaller *SOC* means better denoising effect. Hence, in order to evaluate the denoising effect, we need to consider all the indicators above.

III. RESULTS AND DISCUSSION

For the noised neutron signal x, $x \in \{R\}^N$ with elements $x[n]$, $n = 1, 2, \ldots, N$ and $N = 1024$. The number of compressive sampling is regarded as M, then the corresponding compressive sampling rate is M/N.

As mentioned before, the first two *IMF*s (IMF_1, IMF_2) are noised. Therefore, BPDN algorithm is used to denoise the two IMFs. The results are shown in Fig. 6, where DN is the abbreviation of denoising and $M/N = 0.65$.

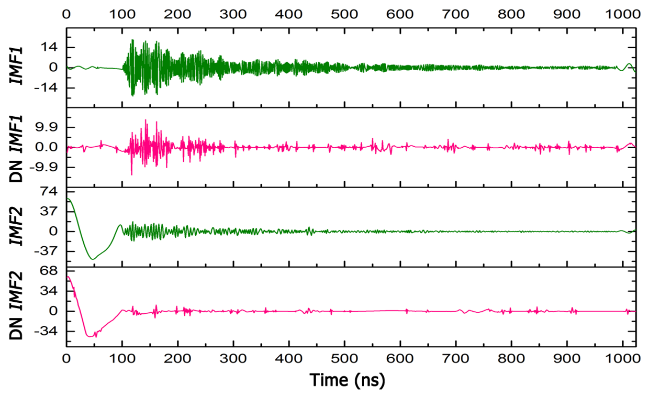

Fig. 6. (Color online) Denoised *IMF*s by EMDCSDN algorithm ($M/N = 0.65$).

Figure 7 shows the EMDCSDN algorithm denoising result of neutron signal. However, this cannot fully reflect the denoising effect, it should be evaluated by the five indicators of *SNR*, *PSNR*, *MSE*, *SOC* and *CC*.

Different compressive sampling rates M/N shall lead to different denoising effects. Figure 8 shows the denoising effects of EMDCSDN algorithm for different M/N. Figure 8 has double Y axis. The left represents the *MSE*, *SOC* and *CC*, and the right one is *SNR*. *SNR* and *CC* increase with M/N, while *MSE* and *SOC* decrease with increasing M/N. The best denoising effect can be seen at $M/N = 0.75$, where *SNR* and *CC* are the biggest, and *MSE* and *SOC* are the smallest, and the denoising effect is the best. However, if we want a lower compressive sampling rate, $M/N = 0.65$ may be a better choice because its denoising effect is very close to $M/N = 0.75$. Here, we choose $M/N = 0.75$.

The EMDCSDN algorithm is compared with four denoising algorithms: (1) EMD Filter (EMDF) that filters the noised *IMF*s directly; (2) Basis Pursuit Denoising (BPDN), compressive sensing denoising problem solved by SPGL1 algorithm; (3) Wavelet Threshold Denoising (WTDN) that denoise signal in wavelet domain with threshold; (4) EMD Wavelet Denoising (EMDWTDN), which uses WTDN to denoise the noised *IMF*s and the reconstruct signal with all *IMF*s. The denoising effects are given in Table 1.

From Table 1, the EMDF algorithm is a simple but less effective algorithm because it also filters out some useful information. As the EMDWTDN algorithm is better than the WTDN algorithm due to the EMD, we think that EMD can improve the denoising effect and the effect of EMDCSDN algorithm confirms this view. Considering all the five indicators, the EMDCSDN algorithm is more effective than the other algorithms due to the EMD and the noised *IMF*s automatic selector, although its processing time is a little longer.

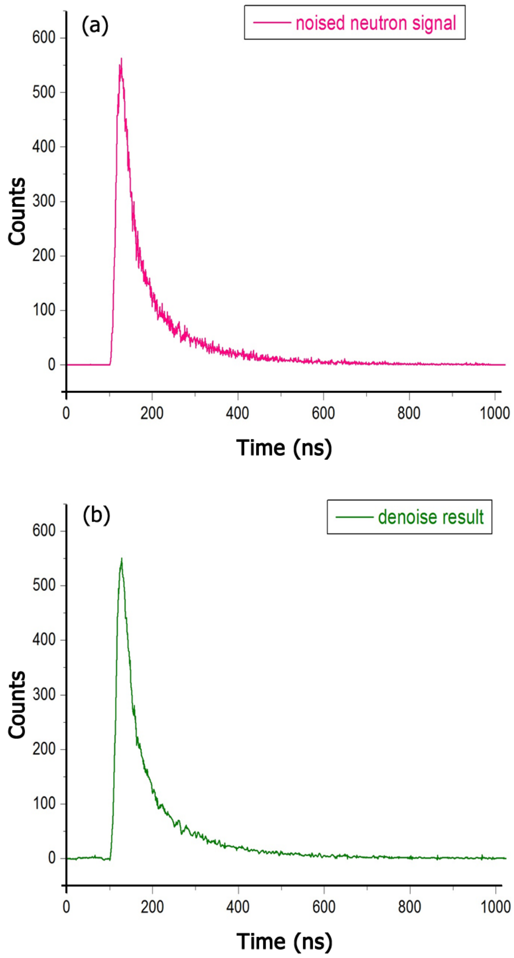

Fig. 7. (Color online) Denoising result of neutron signal ($M/N = 0.65$).

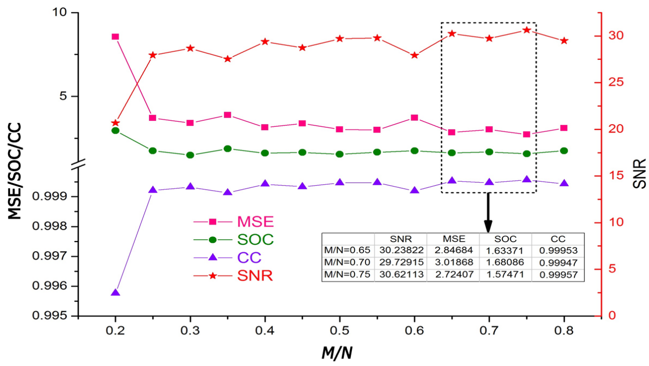

Fig. 8. (Color online) Denoising effect of EMDCSDN algorithm for different M/N.

TABLE 1. Contrast between EMDCSDN and another four denoising algorithms

Algorithm	*SNR*	*PSNR*	*MSE*	*SOC*	*CC*	Processing time (s)
noised neutron signal	24.24559	39.93027	5.67538	5.28919	0.99813	
EMDF	18.16586	33.57995	11.42829	1.12880	0.99249	2.377
BPDN ($M/N = 0.75$)	27.59472	42.93629	3.85956	2.46778	0.99917	1.307
WTDN	28.74912	43.98175	3.37923	0.96627	0.99938	1.588
EMDWTDN	29.48255	44.98517	3.10561	1.99482	0.99944	2.726
EMDCSDN ($M/N = 0.75$)	30.62113	45.89118	2.72407	1.57471	0.99957	3.019

IV. CONCLUSION

A new denoising algorithm, EMDCSDN, has been proposed for noised neutron signal. In fact, it is a modified BPDN algorithm because we only need to denoise the noised *IMF*s that are selected automatically. Thus, it makes our denoising algorithm more specific. It also reduces the compressive sensing reconstruction error. Using five indicators, the EMDCSDN algorithm is more effective than the other denoising algorithms. Moreover, it can reduce the sampling costs. The EMDCSDN algorithm can be used in other denoising applications.

[1] Avdic S, Marinkovic P, Pozzi S A, *et al.* Identification of neutron sources by spectral analysis of pulse height distributions. IEEE T Nucl Sci, 2009, **56**: 2796–2801. DOI: 10.1109/TNS.2009.2022367

[2] Feng P, Liu S Y, Wei B, *et al.* Simulation and experimental study of a random neutron analyzing system with Cf-252 neutron source. Nucl Sci Tech, 2011, **22**: 39–46. DOI: 10.13538/j.1001-8042/nst.22.39-46

[3] Hausladen P A, Blackston M A, Mullens J A, *et al.* Induced-fission imaging of nuclear material. INMM 51st Annual Meeting, Baltimore, Maryland, USA, Jul.11–15, 2010.

[4] Grogan B R, Mihalczo J T, McConchie S M, *et al.* Identification of shielding material configurations using NMIS imaging. INMM 52nd Annual Meeting, Palm Desert, CA, USA, Jul. 17–21, 2011.

[5] Grogan B R and Mihalczo J T. Simulating NMIS imaging and fission-mapping measurements. INMM 52nd Annual Meeting, Palm Desert, CA, USA, Jul. 17–21, 2011.

[6] Wei B, Du K, Ren Y, *et al.* De-noise processing for random signals in nuclear information systems. Journal of Chongqing University, 2008, **31**: 532–540. (in Chinese) DOI: 10.11835/j.issn.1000-582X.2008.05.014

[7] Jin J, Wei B, Feng P, *et al.* A novel de-noising algorithm of fission neutrons signals by photoelectric detection. Laser & Optoelectronics Progress, 2010, **47**: 040702. (in Chinese) DOI: 10.3788/lop47.040702

[8] Davenport M A, Duarte M F, Eldar Y C, *et al.* Compressed sensing: theory and applications. Cambridge (UK): Cambridge University Press, 2012, 1–68.

[9] Qaisar S, Bilal R M, Iqbal W, *et al.* Compressive sensing: from theory to applications, a survey. J Commun Netw, 2013, **15**: 443–456. DOI: 10.1109/JCN.2013.000083

[10] Memmolo P, Esnaola I, Finizio A, *et al.* A new algorithm for digital holograms denoise based on compressed sensing, SPIE Photonics Europe. International Society for Optics and Photonics, Jun. 1, 2012.

[11] Hosseini S H and Shayesteh M G. Compressed sensing for denoise in adaptive system identification. The 20th Iranian Conference on Electrical Engineering ICEE 2012, Tehran, Iran, May 15–17, 2012.

[12] Chen M, Guo S, Wang Y, *et al.* Finger vein image denoise based on compressive sensing. The 4th International Conference on Bioinformatics and Biomedical Engineering (iCBBE 2010), Chengdu, China, Jun.1–4, 2010.

[13] Kang W, Lee E, Chea E, *et al.* Compressive sensing-based image denoise using adaptive multiple sampling and optimal error tolerance. The 38th International Conference on Acoustics, Speech, and Signal Processing (ICASSP), Vancouver, Canada, May 26–31, 2013.

[14] Kang W, Lee E, Kim S, *et al.* Compressive sensing-based image denoise using adaptive multiple samplings and reconstruction error control, SPIE Defense, Security, and Sensing. International Society for Optics and Photonics, Maryland, USA, Jun. 8, 2012.

[15] Zhu L, Zhu Y, Mao H, *et al.* A new method for sparse signal denoise based on compressed sensing. The 2nd International Symposium on Knowledge Acquisition and Modeling, Wuhan, China, Nov. 30–Dec. 1, 2009.

[16] Gemmeke J F and Cranen B. Noise reduction through compressed sensing. The 9th Annual Conference of the International Speech Communication Association. Brisbane, Australia, Sep. 22–26, 2008.

[17] Van Den Berg E and Friedlander M P. Probing the Pareto frontier for basis pursuit solutions. Siam J Sci Comput, 2008, **31**: 890–912. DOI: 10.1137/080714488

[18] Huang N E, Shen Z, Long S R, *et al.* The empirical mode decomposition and the Hilbert spectrum for nonlinear and non-stationary time series analysis. P Roy Soc Lond A Mat, 1998, **454**: 903–995. DOI: 10.1098/rspa.1998.0193

[19] Wu Z and Huang N E. A study of the characteristics of white noise using the empirical mode decomposition method. P Roy Soc Lond A Mat, 2004, **460**: 1597–1611. DOI: 10.1098/rspa.2003.1221